Dynamics of social contagions with heterogeneous adoption thresholds: crossover phenomena in phase transition

New Journal of Physics
The open access journal at the forefront of physics

Deutsche Physikalische Gesellschaft DPG
IOP Institute of Physics

Published in partnership with: Deutsche Physikalische Gesellschaft and the Institute of Physics

OPEN ACCESS

RECEIVED
28 August 2015

REVISED
28 November 2015

ACCEPTED FOR PUBLICATION
17 December 2015

PUBLISHED
12 January 2016

PAPER

Dynamics of social contagions with heterogeneous adoption thresholds: crossover phenomena in phase transition

Wei Wang[1,2], **Ming Tang**[1,2], **Panpan Shu**[1,2] **and Zhen Wang**[3]

[1] Web Sciences Center, University of Electronic Science and Technology of China, Chengdu 610054, People's Republic of China
[2] Big data research center, University of Electronic Science and Technology of China, Chengdu 610054, People's Republic of China
[3] Interdisciplinary Graduate School of Engineering Sciences, Kyushu University, Kasuga-koen, Kasugashi, Fukuoka 816-8580, Japan

E-mail: tangminghan007@gmail.com **and** zhenwang0@gmail.com

Keywords: complex networks, social contagions, phase transition, heterogeneous adoption thresholds

Abstract

Heterogeneous adoption thresholds exist widely in social contagions, such as behavior spreading, but were always neglected in previous studies. To this end, we introduce heterogeneous adoption threshold distribution into a non-Markovian spreading threshold model, in which an individual adopts a behavior only when the received cumulative pieces of behavioral information from neighbors exceeds his adoption threshold. In order to understand the effects of heterogeneous adoption thresholds quantitatively, an edge-based compartmental theory is developed. A two-state spreading threshold model is taken as an example, in which some individuals have a low adoption threshold (i.e., activists) while the remaining ones hold a relatively higher adoption threshold (i.e., bigots). We find a hierarchical characteristic in adopting behavior, i.e., activists first adopt the behavior and then stimulate bigots to adopt the behavior. Interestingly, two types of crossover phenomena in phase transition occur: for a relatively low adoption threshold of bigots, a change from first-order to second-order phase transition can be triggered by increasing the fraction of activists; for a relatively higher adoption threshold of bigots, a change from hybrid to second-order phase transition can be induced by varying the fraction of activists, decreasing mean degree or enhancing network heterogeneity. The theoretical predictions based on the suggested theory agree very well with the simulation results.

1. Introduction

Social contagions are ubiquitous in human society, which generate new scientific challenges for network science [1, 2]. All the researches about sentiments contagion, information spreading and behavior spreading fall into the category of social contagions studies [3, 4]. In particular, behavior spreading, as a representative and essential type of social contagions, has attracted great attention, both theoretically and experimentally [5, 6]. Understanding the spreading mechanisms behind behavior has the potential to not only help us design better anti-virus strategies [7], but also shed new insights into the control of social unrest [1]. Moreover, different from biological contagions (such as epidemic spreading) [8–13], social contagions display one inherent characteristic: social reinforcement effect [7, 14], which usually plays a vital role in the final status of contagions.

To examine social reinforcement effect, some successful models have been proposed [15, 16], most of which assume that all individuals have the same adoption threshold to incorporate such an effect (so-called threshold model). That is to say, each individual adopts the behavior only when the fraction [15] or number [16] of neighbors in the adopted state exceeds his adoption threshold. In this case, the social contagions is a trivial case of Markovian process. By means of numerical simulations and theoretical analysis, it was found that the social reinforcement effect can evidently change the phase transitions of contagion dynamics. More specifically, the final adoption size first grows continuously and then decreases discontinuously with the increase of mean degree when the adoption threshold of all individuals is identical [15]. After this seminal discovery, the role of threshold model and its various underlying mechanisms, in social contagions have been intensively explored, including

the influence of dynamical parameters (e.g., initial seeds and threshold sizes [17, 18]), and topology characteristics (degree–degree correlations [19], clustering [20, 21], community structure [22] as well as multiplexity framework [23, 24]), which are the primary factors in determining the final adoption size and phase transition. Some non-Markovian social contagion models were also proposed to describe the social reinforcement effect [25–27]. For example, in a recent research paper [26], where the social reinforcement was derived from the memory of non-redundant information transmission, it was found that the dependence of final behavior adoption size on information transmission probability changes from being discontinuous to being continuous by varying the dynamical or structural parameters. In [27], Zheng *et al* further verified that social reinforcement plays a crucial role in behavior diffusion on regular graphs and online social networks, which is consistent with early experimental anticipation [28].

Recently, researchers found that the widely existed individual heterogeneity dramatically alters the spreading dynamics. In epidemic spreading, the heterogeneous infectivity and susceptibility can change the outbreak threshold [29, 30]. For information spreading, the heterogeneous waiting and response time may speed up or slow down the velocity of information diffusion [31, 32]. Statistical physicists found that individual heterogeneity can induce the hybrid phase transition [33, 34], which mixes the traditional first-order and second-order transitions, in k-core percolation [35] and bootstrap percolation [17, 36, 37]. In practical behavior spreading, individuals usually show different wills to mimic the behavior, which means that each agent owns his own adoption threshold [38]. Some individuals with low adoption threshold show strong wills to adopt the behavior and act as *activists*. Nevertheless, others with high adoption threshold need to capture more behavioral information before imitation, and they often act as *bigots*. With regard to the difference of adoption threshold, it may be closely related with personal interests, education background, or other personality and social factors [1]. For example, well-educated people are more likely to adopt high-tech products than who lacks the basic education. Similarly, students are more likely to adopt an interesting computer game than housewives.

Unfortunately, there is still absence of systematical understanding about the role of heterogeneous adoption thresholds in social contagions. Aiming to resolve this issue, we will explore how heterogeneous adoption thresholds affect the final adoption size and phase transition of social contagions based on a so-called two-state spreading threshold model, which is a non-Markovian process. Meanwhile, an edge-based compartmental theory is developed for quantitative validation. It is found that heterogeneous adoption thresholds significantly affect the final adoption size, and cause the adopting behavior to present a hierarchical characteristic: activists first adopt the given behavior themselves, and then stimulate bigots to follow this behavior. Noting that such a heterogeneous threshold model results in the existence of first-order, second-order and hybrid phase transitions. And there are two different kinds of crossover phenomena in phase transition for different adoption thresholds of bigots. For a relatively low adoption threshold of bigots, there is a change from first-order to the second-order phase transition, which will be triggered by increasing the fraction of activists; for a relatively higher adoption threshold of bigots, there is a change from hybrid to the second-order phase transition, which can be induced by varying the fraction of activists, decreasing mean degree or enhancing network heterogeneity. In what follows, we will first describe the heterogeneous social contagion model in complex networks, followed by the description of edge-based compartmental theory, and then represent the simulation and analysis results. Finally, we will draw our conclusions.

2. Social contagion model with heterogeneous adoption thresholds

Behavior spreading on complex networks is considered with N nodes and the degree distribution $P(k)$. For the interaction networks, the configuration model [39] is used to avoid the additional influence of degree–degree correlations. Nodes in the network represent individuals and edges between nodes stand for the relationships among individuals. For each individual, a static behavioral adoption threshold is assigned according to a specific distribution function $F(T)$, which is independent of network topology. The larger value of T means that an individual needs to capture more behavioral information from his neighbors before adopting the behavior.

With regard to behavior spreading dynamics, we generalize the spreading threshold model with social reinforcement derived from memory of non-redundant information transmission characteristic [26, 40]. In this model, each individual falls into one of the three states: susceptible (S), adopted (A) and recovered (R) (namely, susceptible–adopted–recovered, SAR model). In the susceptible state, an individual does not adopt the behavior. In the adopted state, an individual adopts the behavior and tries to transmit the behavioral information to his neighbors. In the recovered state, an individual loses interest in the behavior and will not transmit the behavioral information further. Initially, a vanishingly small fraction of individuals ρ_0 are chosen as seeds (adopters) at random, while the others are fixed in the susceptible state.

At each time step, each adopted individual v tries to diffuse the behavioral information to every susceptible neighbor with probability λ. In particular, once the information is transmitted through an edge successfully, it

will never be transmitted again, i.e., only non-redundant information transmission is allowed. Note that an adopted individual can try to transmit the information many times until he entered the recovered state or transmitted the information successfully. If the susceptible neighbor u of v is successfully informed, his cumulative pieces of information m add 1 (i.e., $m = m + 1$). Subsequently, individual u compares the new value of m with his adoption threshold T_u, and becomes an adopter once $m \geqslant T_u$. Obviously, whether an individual adopts the behavior is determined by the cumulative pieces of behavioral information he ever received from distinct neighbors. Thus, the non-Markovian effect is induced in the behavior spreading dynamics. After information transmission, individual v may lose his interest in the behavior with the probability of γ and then moves into the recovered state. Individuals falling into the recovered state will stop from participating in the further behavioral information spreading, and the spreading dynamics terminate when all adopted individuals become recovered. Note that if all individuals have the same adoption threshold $T = 1$, the memory of non-redundant information transmission will disappear. In this case, our model will reduce to the standard SIR model [8], if the adopted state is regarded as the infected state in epidemiology.

3. Edge-based compartmental theory

In order to describe the strong dynamical correlations among the states of neighbors in heterogeneous social contagion model, an edge-based compartmental approach is established herein, which is inspired by [41–43]. Correspondingly, the notations $S(t)$, $A(t)$ and $R(t)$ respectively represent the fraction of individuals in the susceptible, adopted, and recovered states at time step t.

3.1. General adoption threshold distribution

Individual u is set to be in the cavity state, which means that he can receive behavioral information from neighbors but not transmit behavioral information to his neighbors [44]. And $\theta(t)$ is defined to be the probability that individual v has not transmitted the behavioral information to individual u along a randomly chosen edge by time t. Thus, the probability that an individual u with degree k has received m pieces of behavioral information from distinct neighbors by time t can be expressed as

$$\phi_m(k, t) = \binom{k}{m}[\theta(t)]^{k-m}[1 - \theta(t)]^m. \tag{1}$$

Individual u in the susceptible state implies that the cumulative pieces of behavioral information m he received is still less than his adoption threshold T_u. According to the social contagion model in section 2, the adoption threshold and degree are independent. Considering all possible values of m and T_u, it can be obtained that the probability of individual u with degree k being susceptible is

$$s(k, t) = \sum_{T_u} F(T_u) \sum_{m=0}^{T_u - 1} \phi_m(k, t). \tag{2}$$

Combing the degree distribution of a network, it can be known that the fraction of susceptible individuals at time step t is

$$S(t) = \sum_k P(k) s(k, t). \tag{3}$$

Once $\theta(t)$ is known, we can get $S(t)$.

As a neighbor of individual u may be in one of the three states of susceptible, adopted or recovered, $\theta(t)$ can be divided into three cases as

$$\theta(t) = \xi_S(t) + \xi_A(t) + \xi_R(t). \tag{4}$$

And $\xi_S(t)$ [$\xi_A(t)$ or $\xi_R(t)$] denotes the probability that a neighbor of u is in the susceptible (adopted or recovered) state and has not transmitted the behavioral information to individual u up to time t.

Then, let us explore the above three terms. If individual v with degree k' is susceptible initially, he can not transmit the behavioral information to u, but only receive it from other $k' - 1$ neighbors since u in the cavity state. Thus, the probability that individual v has received m pieces of behavioral information by time t is

$$\tau_m(k', t) = \binom{k' - 1}{m}[\theta(t)]^{k'-m-1}[1 - \theta(t)]^m. \tag{5}$$

Taking all possible values of m and T_v into consideration, we can obtain that the probability of individual v remaining in susceptible state is (similar to equation (2))

$$\Theta(k', t) = \sum_{T_v} F(T_v) \sum_{m=0}^{T_v-1} \tau_m(k', t). \tag{6}$$

The probability of an edge connecting an individual with degree k' is $k'P(k')/\langle k\rangle$ for uncorrelated networks, where $\langle k\rangle$ is the mean degree. Thus, it can be obtained that

$$\xi_S(t) = \frac{\sum_{k'} k'P(k')\Theta(k', t)}{\langle k\rangle}. \tag{7}$$

Subsequently, we turn to the expressions of $\xi_A(t)$ and $\xi_R(t)$. Once the behavioral information is transmitted through an edge with probability λ, the edge will no longer satisfy the definition of $\theta(t)$. Thus, the decrease of the fraction from $\theta(t)$ to $1 - \theta(t)$ is $\lambda\xi_A(t)$, which can be expressed as

$$\frac{\mathrm{d}\theta(t)}{\mathrm{d}t} = -\lambda\xi_A(t). \tag{8}$$

For the growing of $\xi_R(t)$, two conditions must be met simultaneously. At time t, the behavioral information does not transmit through an edge with probability $1 - \lambda$, and the adopted individual enters recovered state with probability γ. Then

$$\frac{\mathrm{d}\xi_R(t)}{\mathrm{d}t} = \gamma(1 - \lambda)\xi_A(t). \tag{9}$$

Based on equations (8) and (9), and the initial conditions of $\theta(0) = 1$ and $\xi_R(0) = 0$, we can get the integration constant $\gamma(1 - \lambda)/\lambda$ and

$$\xi_R(t) = \frac{\gamma[1 - \theta(t)](1 - \lambda)}{\lambda}. \tag{10}$$

Inserting equations (7) and (10) into (4), the following expression can be obtained that

$$\xi_A(t) = \theta(t) - \frac{\sum_{k'} k'P(k')\Theta(k', t)}{\langle k\rangle} - \frac{\gamma[1 - \theta(t)](1 - \lambda)}{\lambda}. \tag{11}$$

Substituting equation (11) into (8), we can get the time evolution of $\theta(t)$ in detail

$$\frac{\mathrm{d}\theta(t)}{\mathrm{d}t} = -\lambda[\theta(t) - \frac{\sum_{k'} k'P(k')\Theta(k', t)}{\langle k\rangle}] + \gamma[1 - \theta(t)](1 - \lambda). \tag{12}$$

Susceptible individuals move into the adopted states once they adopt the behavior. Meanwhile, the adopted individuals may lose interest in the behavior and become recovered. Thus, we can easily get the evolution of adopted and recovered individuals as

$$\frac{\mathrm{d}A(t)}{\mathrm{d}t} = -\frac{\mathrm{d}S(t)}{\mathrm{d}t} - \gamma A(t) \tag{13}$$

and

$$\frac{\mathrm{d}R(t)}{\mathrm{d}t} = \gamma A(t), \tag{14}$$

respectively. Equations (1)–(3) and (12)–(14) give us a complete and general description of heterogeneous social contagions, from which the fraction in each state at arbitrary time step can be calculated. When $t \to \infty$, we can get the final adoption size $R(\infty)$.

3.2. Binominal adoption threshold distribution

In this subsection, we pay attention to the behavior adoption threshold with a binominal distribution $F(T)$. More specifically, a fraction of individuals p has a relatively low adoption threshold T_a, whereas the remaining ones have a higher adoption threshold T_b. $F(T)$ can be expressed as

$$F(T) = \begin{cases} T_a, & \text{with probability } p, \\ T_b, & \text{with probability } 1 - p. \end{cases} \tag{15}$$

For simplicity, the values of adoption thresholds are defined as $T_a = 1$ and $T_b \geqslant 1$. Individuals with low adoption threshold T_a are considered as *activists*, while those with high adoption threshold T_b are regarded as *bigots*. We herein name this kind of social contagion model as *two-state spreading threshold model*. And the edge-based compartmental theory is utilized to analyze the two-state spreading threshold model by substituting equation (15) into the corresponding equations, thus obtaining the value of $S(t)$, $A(t)$ and $R(t)$. Particularly, we rewrite equations (2) and (6) as

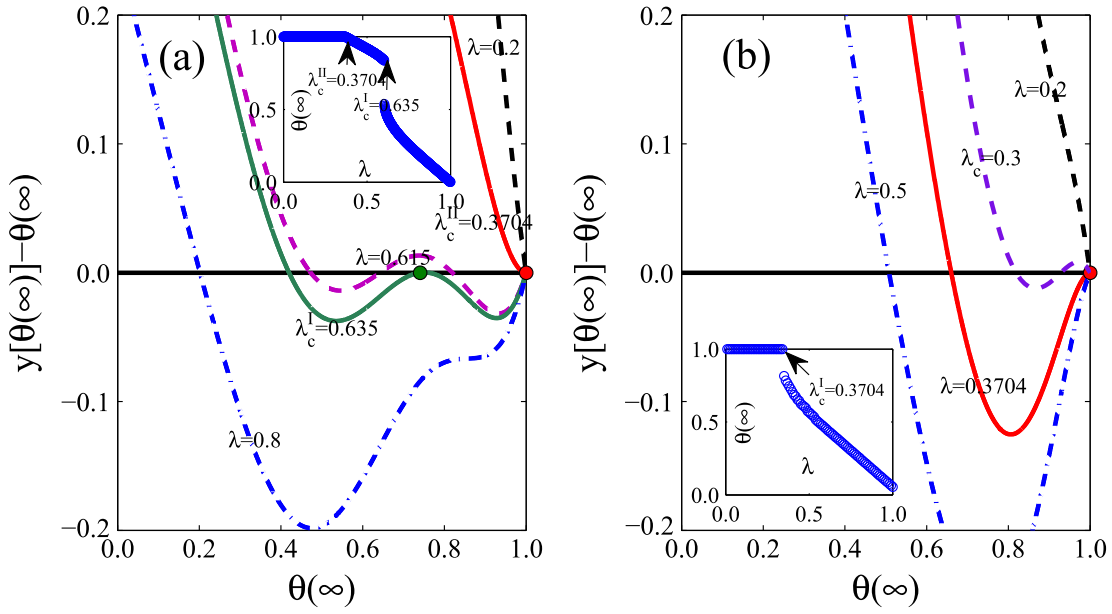

Figure 1. Illustration of graphical solutions of equation (21) when $T_b = 4$ (a) and $T_b = 2$ (b) on random regular networks. In (a) and (b), the black solid lines represent the horizontal axis and the red and green dots denote the tangent points. The inset of (a) and (b) shows the physically meaningful solutions of equation (21) when $T_b = 4$ and $T_b = 2$, respectively. And the arrows indicate critical transmission probabilities. The fixed points of equation (21) are the intersections between the curve and horizontal axis. Other parameters are defined as $p = 0.3$ and $\langle k \rangle = 10$.

$$s(k, t) = p\theta(t)^k + (1 - p)\sum_{m=0}^{T_b-1}\phi_m(k, t), \tag{16}$$

and

$$\Theta(k', t) = p\theta(t)^{k'-1} + (1 - p)\sum_{m=0}^{T_b-1}\tau_m(k', t), \tag{17}$$

respectively. At time t, the fractions of susceptible individuals in the activist and bigot populations are given by

$$S_a(t) = \sum_k P(k)\theta(t)^k, \tag{18}$$

and

$$S_b(t) = \sum_k P(k)\sum_{m=0}^{T_b-1}\phi_m(k, t), \tag{19}$$

respectively. Considering the fractions of the activist and bigot populations, the density of susceptible individuals at time step t can also be written as

$$S(t) = pS_a(t) + (1 - p)S_b(t). \tag{20}$$

Another issue concerned in the paper is the effects of heterogeneous adoption threshold on phase transition. To analyze the phase transition, we address the fixed point (root) of equation (12) at the steady state (i.e., $t \to \infty$) with equation (17). That is the fixed point of

$$\theta(\infty) = y[\theta(\infty)], \tag{21}$$

where

$$y[\theta(\infty)] = \frac{\sum_{k'} k'P(k')\Theta(k', \infty)}{\langle k \rangle} + \frac{\gamma[1 - \theta(\infty)](1 - \lambda)}{\lambda}. \tag{22}$$

From figure 1(a), it can be seen that the number of nontrivial roots is 0, 1 or 3 when $T_b \geqslant 3$. For the case of $T_b = 2$, the number of nontrivial roots is 0, 1 or 2 (see figure 1(b)).

3.2.1. Case of $T_b \geqslant 3$

In this subsection, we discuss the case of $T_b \geqslant 3$. For the given P(k), p and γ, equation (21) has only one trivial solution $\theta(\infty) = 1$ when λ is small. With the increase of λ, $\theta(\infty)$ decreases continuously to a nontrivial solution $\theta(\infty) < 1$ first (see example in figure 1(a)), which means that $R(\infty)$ grows continuously first. That is

to say, there is a second-order (continuous) phase transition. By setting $\theta(\infty)$ and y $[\theta(\infty)]$ tangent at $\theta(\infty) = 1$ [34, 45], we can get the continuous critical information transmission probability as

$$\lambda_c^{II} = \frac{\gamma\langle k\rangle}{p(\langle k^2\rangle - \langle k\rangle) - (1-\gamma)\langle k\rangle}, \tag{23}$$

where $\langle k\rangle$ and $\langle k^2\rangle$ are the first and second moments of degree distribution, respectively. The critical value λ_c^{II} separates the local behavior adoption from the global behavior adoption. A local behavior adoption means that the behavior can be adopted by few individuals, and a global behavior adoption represents that the behavior can be adopted by a finite fraction of individuals (i.e., the final adoption size is proportional to the number of individuals in the network). From equation (23), it is discovered that the emergence of global behavior adoption is determined by the network topology (i.e., degree distribution), the fraction of activists p and the recovery probability γ. The global behavior adoption is more likely to occur (i.e., a lower λ_c^{II}) in scale-free networks with divergent second moment degree distribution (i.e., $\langle k^2\rangle \to \infty$). Increasing the value of p can facilitate the global behavior adoption (i.e., a lower λ_c^{II}). When $p = 1$, equation (23) returns to the case of epidemic outbreak threshold [43].

Fixing all the parameters except p, as similar to equation (23), we get the continuous critical fraction of activists as

$$p_c^{II} = \frac{\gamma\langle k\rangle}{\lambda(\langle k^2\rangle - \langle k\rangle)} + \frac{(1-\gamma)\langle k\rangle}{\langle k^2\rangle - \langle k\rangle}. \tag{24}$$

From equation (24), it can be known that an enough fraction of activists are necessary for triggering the global behavior adoption, and p_c^{II} decreases with the increase of network heterogeneity, p and λ. By setting $\gamma = 0$ in equation (24), another critical proportion of activists $p_c^{\star}$ can be obtained, below which any values of λ can not trigger the global behavior adoption, and it is

$$p_c^{\star} = \frac{\langle k\rangle}{\langle k^2\rangle - \langle k\rangle}. \tag{25}$$

It is worth noting that equation (25) is the same with network's percolation condition [45], which means that the global behavior adoption is possible only when the activists percolate the entire network (i.e., activists can form a finite connected cluster).

As shown in figure 1(a), three nontrivial roots of equation (21) occur when λ is large enough (see figure 1(a) for $\lambda = 0.615$). This phenomenon is caused by the bigots, since equation (21) has at most one nontrivial root when the bigots are absent [26]. In this case, the meaningful solution will be given by the largest stably root (since only this value can be achieved physically). For $\lambda = \lambda_c^{I} = 0.635$, the tangent point is the solution. For $\lambda > \lambda_c^{I}$, the meaningful solution is the only stably fixed point. The meaningful solution of equation (21) changes abruptly to a small value from a relatively large value at λ_c^{I} (see the insert figure 1(a)), resulting in a discontinuous growth of $R(\infty)$. Based on the bifurcation theory [46], the discontinuous critical information transmission probability can be obtained as follows

$$\lambda_c^{I} = \frac{\gamma}{\Delta + \gamma - 1}, \tag{26}$$

where

$$\Delta = \frac{\sum_{k'} k' P(k') \frac{d\Theta(k',\infty)}{d\theta(\infty)}|_{\theta_s(\infty)}}{\langle k\rangle},$$

and $\theta_s(\infty)$ is the fixed point of equation (21). Combining equations (5) and (17), we can get that

$$\frac{d\Theta(k',\infty)}{d\theta(t)} = p(k'-1)\theta(\infty)^{k'-2} + (1-p)\mathcal{X}, \tag{27}$$

where

$$\mathcal{X} = \sum_{m=0}^{T_b-1}\binom{k'-1}{m}\{(k'-m-1)\theta(\infty)^{k'-m-2}[1-\theta(\infty)]^m - m\theta(\infty)^{k'-m-1}[1-\theta(\infty)]^{m-1}\}.$$

Using the analytical method similar to equation (26), it is obtained that the discontinuous critical fraction of activists can be expressed as

$$p_c^{I} = \frac{\lambda(1-\mathcal{Y}) + \gamma(1-\lambda)}{\lambda(\mathcal{Z}-\mathcal{Y})}, \tag{28}$$

where

$$\mathcal{Y} = \frac{\sum_{k'} k' P(k') \mathcal{X}}{\langle k \rangle}$$

and

$$\mathcal{Z} = \frac{\sum_{k'} k'(k'-1) P(k') \theta^{k'-2}}{\langle k \rangle}.$$

From the above analysis, we find that $R(\infty)$ versus λ or p first grows continuously and then follows a discontinuous fashion. And the continuous and discontinuous growthes of $R(\infty)$ are caused by the activists and bigots, respectively, which can be regarded as hybrid phase transition [47] from the perspective of statistical physics, due to its mixture of the traditional first-order and second-order transitions. Note that the hybrid phase transition can change to a second-order phase transition. Numerically solving equations (21) and (26), and the following equation

$$\frac{\mathrm{d}^2 y[\theta(\infty)]}{\mathrm{d}\theta^2(\infty)} = 0, \tag{29}$$

we can learn the condition under which the hybrid phase transition disappears.

3.2.2. Case of $T_b = 2$

We study the special case of $T_b = 2$ in this subsection. As shown in figure 1(b), for any λ $y[\theta(\infty)]$ can only tangent to $\theta(\infty)$ when $\theta(\infty) = 1$, and can not tangent to other $\theta(\infty) < 1$. In addition, equation (21) has 1 or 2 nontrivial fixed points. These phenomena means that the meaningful solution of equation (21) jumps to another one at the critical information transmission probability (see the inset of figure 1(b)). As a result, $R(\infty)$ increases discontinuously versus λ. The critical information transmission probability can be acquired in the similar way as when $T_b = 3$. The values of λ_c^{II} and λ_c^{I} can be obtained from equation (23), since $y[\theta(\infty)]$ can only tangent to $\theta(\infty)$ when $\theta(\infty) = 1$. Numerically solving equations (21), (26) and (29), we can get the condition under which the first-order phase transition changes to a second-order phase transition.

4. Numerical verification

In the study, extensive simulations are conducted for one two-state spreading threshold model on uncorrelated networks. Unless otherwise specified, the network size, mean degree and recovery probability are of $N = 10\,000$, $\langle k \rangle = 10$ and $\gamma = 1.0$, respectively. At least 2×10^3 independent dynamical realizations on a fixed network are used to calculate the pertinent average values, which are further averaged over 100 network realizations.

The *relative variance* v_R is applied numerically to determine the size-dependent critical values, such as, λ_c^{I}, λ_c^{II}, p_c^{I} and p_c^{II}. The relative variance of $R(\infty)$ is defined as

$$v_R = \frac{\langle R(\infty) - \langle R(\infty) \rangle \rangle^2}{\langle R(\infty) \rangle^2}, \tag{30}$$

where $\langle \cdots \rangle$ denotes ensemble averaging. The value of v_R exhibits peaks at the phase transition, which announce the phase transition [48]. We determine the critical value $\omega_c \in \{\lambda_c^{\mathrm{I}}, \lambda_c^{\mathrm{II}}, p_c^{\mathrm{I}}, p_c^{\mathrm{II}}\}$ as the value of λ or p where the relative variance reaches its maximum

$$\omega_c = \arg\{\max v_R\}. \tag{31}$$

In the remaining of this section, we separately discuss the effects of dynamical parameters [e.g., the fraction of activists p, the information transmission probability λ and the adoption threshold of bigots T_b] and the topological parameters of networks (the mean degree $\langle k \rangle$ and degree distribution $P(k)$).

4.1. Effects of dynamical parameters

To be illustrative, we first focus on random regular networks (RRNs). Figure 2(a) shows the time evolution of the fraction of adopted individuals $A_a(t)$ and $A_b(t)$ in the activist and bigot populations with different behavioral information transmission probabilities λ. It is found that a hierarchical characteristic of behavior adoption is caused by heterogeneous adoption thresholds. That is to say, activists with low T_a first adopt the behavior and then stimulate the bigots with T_b to adopt the behavior. With a relatively small $\lambda = 0.5$, $A_a(t)$ shows a small peak, and can not stimulate many bigots to adopt the behavior ($A_b(t)$ does not see an obvious peak). With a relatively large $\lambda = 0.7$, $A_a(t)$ shows a large peak, and further leads to the emergence of a large

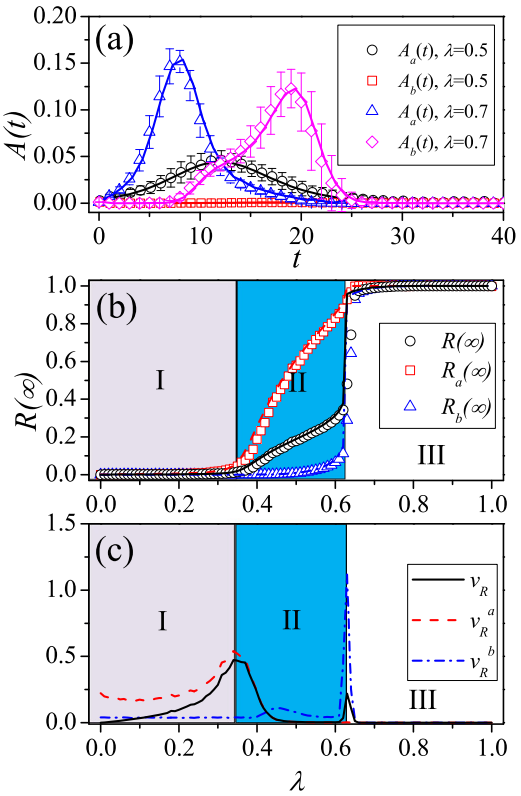

Figure 2. Binary spreading threshold model on random regular networks. (a) Average density of adopted individuals $A_a(t)$ and $A_b(t)$ versus time t for the activist and bigot with different information transmission probability λ. The error bars indicate the standard deviations. To the full, activist and bigot populations, (b) the final adoption size $R(\infty)$ and (c) relative variance v_R versus λ, respectively. In figures (a) and (b), symbols represent the simulated results, and the lines are the corresponding theoretical predictions from equations (12)–(14) and (16)–(20). Lines in (c) are the simulation results of v_R. In (b) and (c), the vertical lines are the critical continuous and discontinuous information transmission probabilities, which are denoted as λ_c^{II} and λ_c^{I}, respectively. The theoretical values of λ_c^{II} and λ_c^{I} can be gotten from equations (23) and (26), respectively. The theoretical (numerical) values of λ_c^{II} and λ_c^{I} separate (b) and (c) into three regions. Region I, only a vanishingly small fraction of individuals can be exposed to adopt the behavior; region II, only a finite fraction of activists adopt the behavior; region III, a finite fraction of activists and bigots adopt the behavior. Other parameters are set to be $N = 10\,000, p = 0.3$ and $T_b = 4$.

peak for $A_a(t)$. The heterogeneous adoption threshold distribution may be used to understand some real-world hierarchical phenomena of behavior adoption, such as the adoption of Skype serves [38]. The time evolution can be well predicted by our edge-based compartmental theory.

From figure 2(b), it can be seen that $R(\infty)$ versus λ shows a hybrid phase transition, which means that $R(\infty)$ first grows continuously and then follows a discontinuous fashion. The continuous and discontinuous phase transitions are caused by activists and bigots, respectively. Similar to [26], the discontinuous growth of $R(\infty)$ is caused by those bigots in the subcritical state who adopt the behavior simultaneously. An individual in such a state has received the behavioral information but has not yet adopted the behavior, and the pieces of information from distinct neighbors is precisely one less than his adoption threshold. The theoretical (numerical) values of λ_c^{II} and λ_c^{I} separate figures 2(b) and (c) into three regions. The theoretical values of λ_c^{II} and λ_c^{I} can be gotten from equations (23) and (26), respectively. In region I, with $\lambda \leqslant \lambda_c^{\mathrm{II}}$, both activist and bigot populations adopt the behavior locally (i.e., only a vanishingly small fraction of individuals adopted the behavior). In region II, with $\lambda_c^{\mathrm{II}} < \lambda \leqslant \lambda_c^{\mathrm{I}}$, activists adopt the behavior globally (i.e., a finite fraction of activists adopted the behavior) and bigots adopt the behavior locally. In region III with $\lambda > \lambda_c^{\mathrm{I}}$, both the activists and bigots adopt the behavior globally. The numerical values of λ_c^{II} and λ_c^{I} can be obtained by observing v_R in figure 2(c). For instance, v_R has two peaks, which means that two phase transitions occur [48]. And the first peak appears at λ_c^{II}, while the second peak locates at λ_c^{I}. Note that the first (second) peak of v_R shares the same location with the maximal peak of activist population v_R^a (bigots population v_R^b). In all, λ_c^{I}, λ_c^{II} and $R(\infty)$ can be well predicted by our edge-based compartmental theory.

As shown in figure 3, $R(\infty)$ and the phase transition are significantly influenced by the adoption threshold of bigots T_b. And $R(\infty)$ decreases with T_b, since a larger value of T_b means the bigots need to be exposed to more information before adopting the behavior. The phase transition is continuous when $T_b = 1$. In this case, our model reduces to the SIR model [8]. The phase transition is also continuous when $T_b \geqslant 6$, since there are not

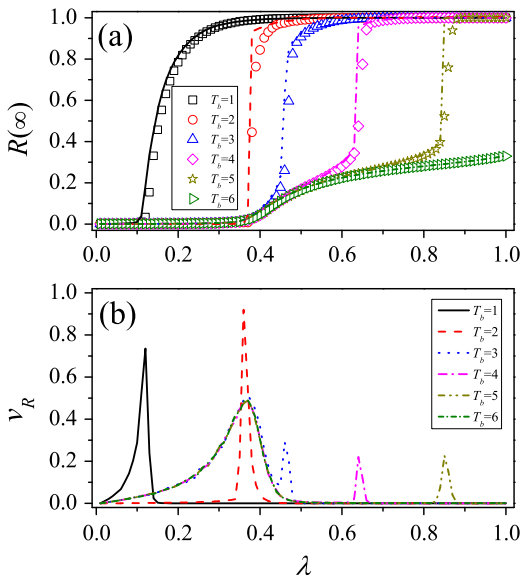

Figure 3. Effects of bigots' adoption threshold on two-state spreading threshold model. (a) $R(\infty)$ and (b) ν_R versus λ with different T_b. In figure (a), symbols represent the simulated results, and the lines are the theoretical predictions from equations (12)–(14) and (16)–(20). In figure (b), lines are the simulation results of ν_R, and we plot the value of $\nu_R/20$ when $T_b = 2$. Other parameters are defined as $N = 10\,000$ and $p = 0.3$.

enough activists to persuade bigots to adopt the behavior simultaneously. For the case of $T_b = 2$, $R(\infty)$ shows a first-order phase transition, because the bigots are likely to enter subcritical states and adopt the behavior simultaneously. A hybrid phase transition emerges with other values of T_b (i.e., $2 < T_b < 6$). As discussed in section 3.2, the type of phase transition is verified by bifurcation analysis of equation (21). As shown in figure 3(b), the simulated values of λ_c^{II} and λ_c^{I} are located by studying ν_R versus λ. For the second-order phase transition, ν_R has only one peak (see $T_b = 1$ and $T_b = 6$ in figure 3(b)). Similarly, ν_R also has only one peak for the first-order phase transition (see $T_b = 2$ in figure 3(b)). For the hybrid phase transition, ν_R has two peaks (see $3 \leqslant T_b \leqslant 5$ in figure 3(b)). Our theoretical predictions of $R(\infty)$ agree well with the simulation results, except for λ close to the critical information transmission probability. The deviations between our predictions and simulation are mainly derived from the finite-size effects of networks, as shown in figure 4. The deviations of $R(\infty)$, λ_c^I and λ_c^{II} between the simulated and theoretical results decrease with network size N.

Then, we observe $R(\infty)$ versus p for different λ in figure 5. We find that $R(\infty)$ increases with p. By bifurcation analysis of equation (21), a continuous growth of $R(\infty)$ is observed with a relatively small λ (e.g., $\lambda = 0.5$), and the hybrid phase transition occurs with a relatively large λ (e.g., $\lambda = 0.7$ and 0.8). The numerical values of λ_c^{I} and λ_c^{II} are located by studying ν_R (see figure 5(b)). Again, the theoretical and numerical results agree well.

From the above analysis, it can be obtained that both λ and p markedly affect $R(\infty)$ and phase transition. Thus, $R(\infty)$ and the phase transition on parameter plane (λ, p) when $T_b = 4$ are further investigated in figure 6. Obviously, $R(\infty)$ increases with λ and p. According to the type of phase transition, the parameter plane (λ, p) is divided into four different regions by three vertical lines. The first vertical line can be gotten from equation (25), and the other two can be predicted by solving equations (21), (26) and (29). In region I ($p \leqslant p_c^\star = 1/9$), there are a few activists, who can not percolate the entire population. Thus, no matter what the value of λ is, activists can not be made to adopt the behavior globally. When $p > p_c^\star$, the global behavior adoption becomes possible, and a crossover phenomenon, which means that the phase transition changes from being hybrid to being second-order, occurs in the phase transition. Meanwhile, the local and global behavior adoptions are separated by the red solid curve (i.e., λ_c^{II}). In region II ($1/9 < p \leqslant 0.15$), the relatively few activists lead to the continuous phase transition. In this region, $R(\infty)$ grows continuously versus λ for a given p, and a finite fraction of individuals adopt the behavior above λ_c^{II}. With the increase of p, in region III ($0.15 < p \leqslant 0.5$), the hybrid phase transition occurs, i.e., $R(\infty)$ first grows continuously with λ and then follows by a discontinuous pattern. A finite fraction of activists adopt the behavior above λ_c^{II}, and further induce the bigots to adopt the behavior simultaneously above λ_c^{I} (see black curves obtained from equation (26)). In region IV ($p > 0.5$), half of the neighbors of bigots are activists. Once these activists adopt the behavior, the bigots will gradually adopt the behavior. Thus, $R(\infty)$ grows continuously and a finite fraction of individuals adopt the behavior above λ_c^{II} (see red curves). Our theoretical predictions of λ_c^{II}, λ_c^I and $R(\infty)$ agree well with the numerical predictions.

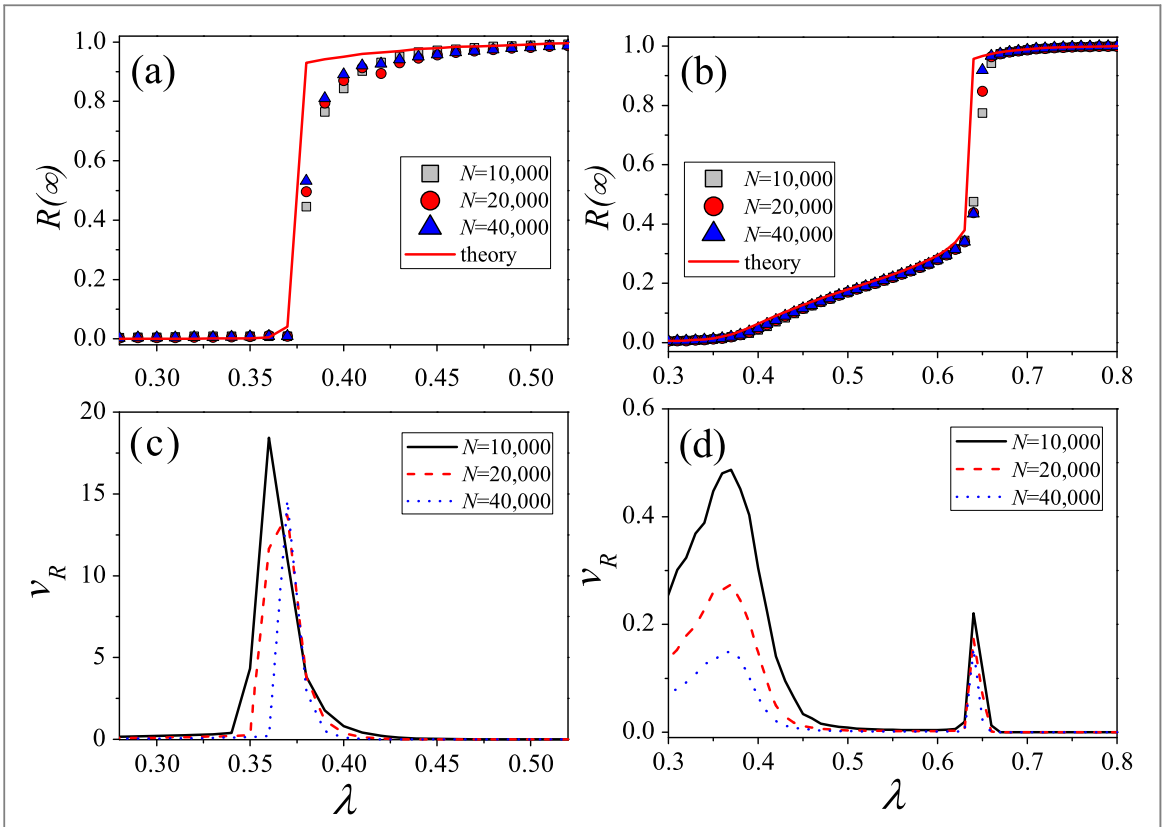

Figure 4. Finite-size effects on the two-state spreading threshold model when $p = 0.3$. (a) $R(\infty)$ and (c) ν_R versus λ when $T_b = 2$ with different network size N. (b) $R(\infty)$ and (d) ν_R versus λ when $T_b = 4$ with different N. The lines in (a) and (b) are the theoretical predictions from equations (12)–(14) and (16)–(20). The lines in (c) and (d) are the simulation results of ν_R.

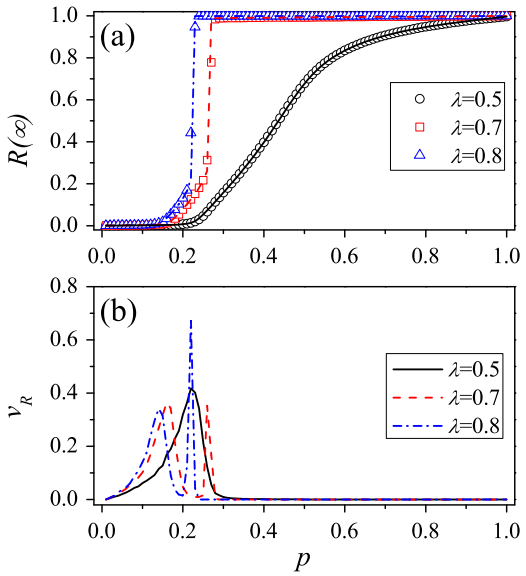

Figure 5. Effects of the fraction of activists on two-state spreading threshold model. (a) $R(\infty)$ and (b) ν_R as a function of p with different λ. In figure (a), symbols represent the simulated results, and the lines are the theoretical predictions from equations (12)–(14) and (16)–(20). Lines in (b) are the simulation results of ν_R. We set other parameters to be $N = 10\,000$ and $T_b = 4$.

It can be seen in figure 3 that $R(\infty)$ increases discontinuously with λ when $T_b = 2$, thus $R(\infty)$ and phase transition on parameter plane $p\lambda$ when $T_b = 2$ is explored in figure 7. And we find another crossover phenomenon in the phase transition: a change from being first-order to being second-order. Here, what is similar to figure 6 is that the plane is divided into three regions: region I ($p \leqslant 1/9$), the local behavior adoption region, in which only a vanishingly small fraction of individuals adopt the behavior; region II ($1/9 < p \leqslant 0.42$)

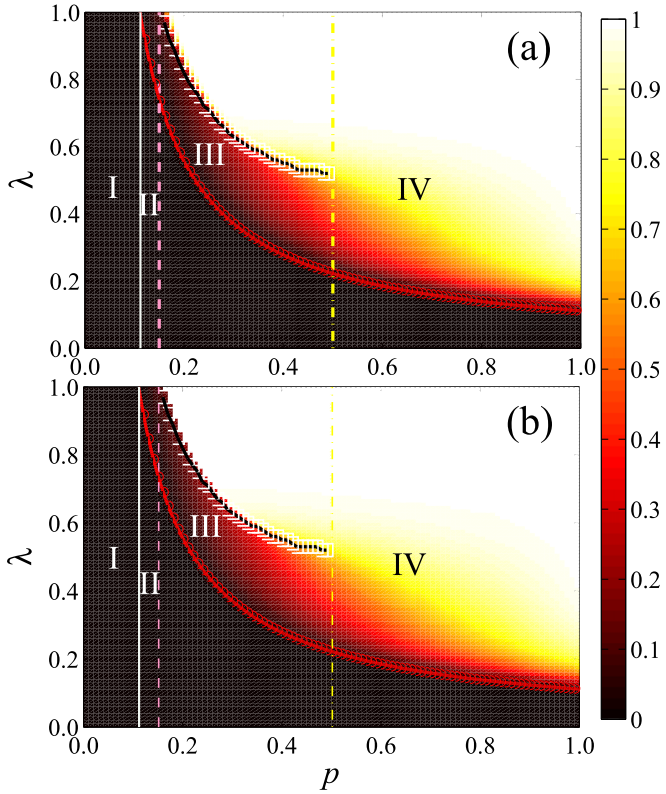

Figure 6. Dependence of $R(\infty)$ on p and λ on random regular networks. Color-coded values $R(\infty)$ are obtained from numerical simulations (a) and theoretical solutions (b) in the parameter plane (p, λ), and the theoretical predictions are the solutions of equations (12)–(14) and (16)–(20). The plane are divided into four regions by three vertical lines, of which the first line can be gotten from equation (25) and the other two are predicted by solving equations (21), (26) and (29). In region I, only a vanishingly small fraction of individuals can be exposed to adopt the behavior (i.e., local behavior adoption). Both the regions II and IV show a continuous phase transition, whereas region III exhibits a hybrid phase transition. The red circles (red solid curve) and white squares (black dished curve) are the continuous and discontinuous simulated (theoretical) critical information transmission probability, respectively. Moreover, other parameters are defined as $N = 10\,000$, $p = 0.3$ and $T_b = 4$.

shows a first-order phase transition, where a finite fraction of individuals adopt the behavior simultaneously above λ_c^{I} (red dished lines); region III ($p > 0.42$) exhibits a second-order phase transition, in which $R(\infty)$ increases continuously versus λ. The type of phase transition is verified by bifurcation analysis.

4.2. Effects of network topological parameters

We turn to investigate the effects of network topological parameters, including the mean degree and degree heterogeneity, on the two-state spreading threshold model. We first examine RRNs with different values of mean degree $\langle k\rangle$. As shown in figure 8, the behavior spreads easier for a greater value of $\langle k\rangle$. For the case of $T_b = 2$, the type of phase transition is not altered by $\langle k\rangle$, i.e., $R(\infty)$ always increases discontinuously with λ (see figure 8(a)). For the case of $T_b = 4$ in figure 8(b), the phase transition changes from a hybrid type for a relatively large mean degree (e.g., $\langle k\rangle = 10$) to a continuous type for a small value of $\langle k\rangle = 5$. We verify the type of phase transition by bifurcation analysis. The numerical critical values are located by studying v_R in figures 8(c) and (d). The theory can predict simulation results $R(\infty)$ very well except for λ close to the critical points. The deviations are induced by the finite-size effects of networks.

We next study the effects of network heterogeneity. To build the heterogeneous networks, the uncorrelated configuration model with power-law degree distributions $P(k) \sim k^{-\gamma_D}$ is used, where the mean degree $\langle k\rangle = 10$ and the maximum degree $k_{\max} \sim \sqrt{N}$ [39]. The network heterogeneity increases with the decrease of γ_D.

In the case of $T_b = 4$, we find that the global behavior adoption more likely to occur (i.e., lower λ_c^{II}) in heterogeneous networks, due to the existence of hubs in heterogeneous networks [49], as shown in figure 9. Meanwhile, in strong heterogeneous networks a large number of individuals with small degrees are difficult to adopt the behavior, so $R(\infty)$ is smaller at large λ. For example, $R(\infty)$ at $\lambda = 0.7$ is obviously smaller on scale-free networks with $\gamma_D = 2.5$ than that on RRNs. By bifurcation analysis of equation (21), it is discovered that the hybrid phase transition disappears for strong heterogeneous networks (e.g., $\gamma_D = 2.5$ and 3.0 in figure 9). That is to say, network heterogeneity leads to the crossover phenomenon: a change from hybrid to second-order

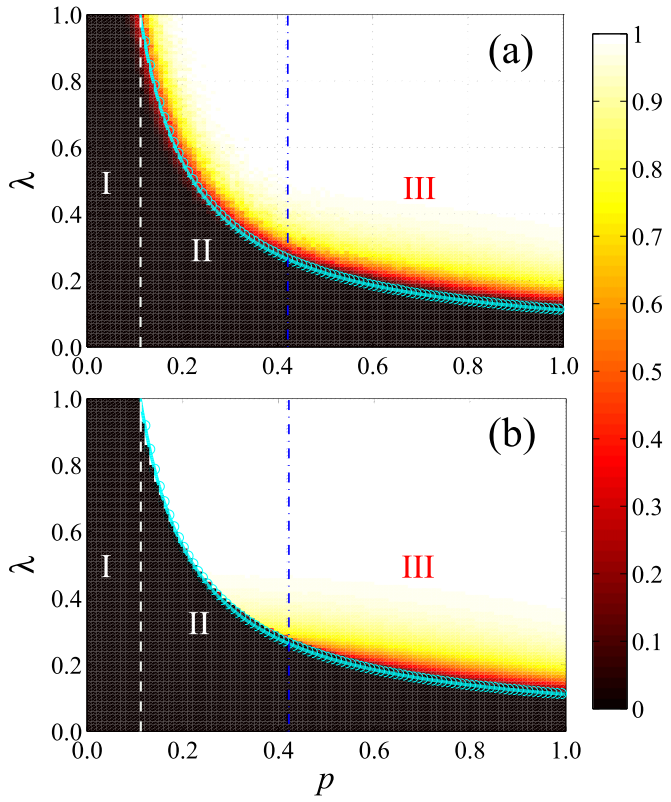

Figure 7. Dependence of $R(\infty)$ on p and λ. Color-coded values $R(\infty)$ from numerical simulations (a) and theoretical solutions (b) in the parameter plane (p, λ), and the theoretical predictions are the solutions of equations (12)–(14) and (16)–(20). Two vertical lines separate the plane into three regions, the former line is predicted by equation (25) and the latter line is predicted by numerically solving equations (21), (26) and (29). In region I, only a vanishingly small fraction of individuals can be exposed to adopt the behavior (i.e., local behavior adoption). Region II shows a discontinuous phase transition, while region III exhibits a continuous phase transition. The blue circles and blue dished solid curve are the simulated and theoretical critical information transmission probabilities, respectively. Moreover, we set other parameters as $N = 10\,000, p = 0.3$ and $T_b = 2$.

phase transition. Moreover, the numerical critical values are further located by observing ν_R in figure 9(b). Evidences in terms of the quantities $R(\infty)$, λ_c^I and λ_c^{II}, which support our edge-based compartmental theory.

For the case of $T_b = 2$ (see figure 10), we find the similar phenomenon of final behavior adoption size $R(\infty)$ increases (decreases) with network heterogeneity when λ is small (large). Based on bifurcation theory, we find that the system has the first-order phase transition, which denotes that network heterogeneity does not alter the phase transition. As shown in figure 10(b), we locate the numerical critical values by studying ν_R. The deviations between the theoretical predictions and simulation results are mainly caused by the finite-size effects of networks.

5. Conclusions

Understanding social contagion dynamics in human populations is extremely challenging. In practical behavior spreading, individuals usually display different criterions (wills) to adopt the behavior. That is to say, the heterogeneity of adoption thresholds do exist, but its effects on social contagions have not been verified straightforwardly. To fill this gap, we proposed a non-Markovian behavior spreading model, in which individuals have different adoption thresholds, to explore how heterogeneous adoption thresholds affect the final adoption size and phase transition. An edge-based compartmental theory is developed to quantificationally describe this model, and the suggested theory is verified by a large number of simulations.

In the paper, we mainly focused on the so-called two-state spreading threshold model, in which a fraction of individuals p have the adoption threshold $T_a = 1$ and are acted as activists, and the remaining ones have a higher adoption threshold T_b and are regarded as bigots. We systematically studied the effects of dynamical and topological parameters on this model. To investigate the effects of dynamical parameters directly, we study the spreading dynamics on RRNs. It is found that heterogeneous adoption thresholds markedly affect the final adoption size, i.e., $R(\infty)$ decreases with T_b. The heterogeneous adoption thresholds also induce a hierarchical characteristic in behavior adoption: activists first adopt the behavior and then stimulate bigots to adopt the

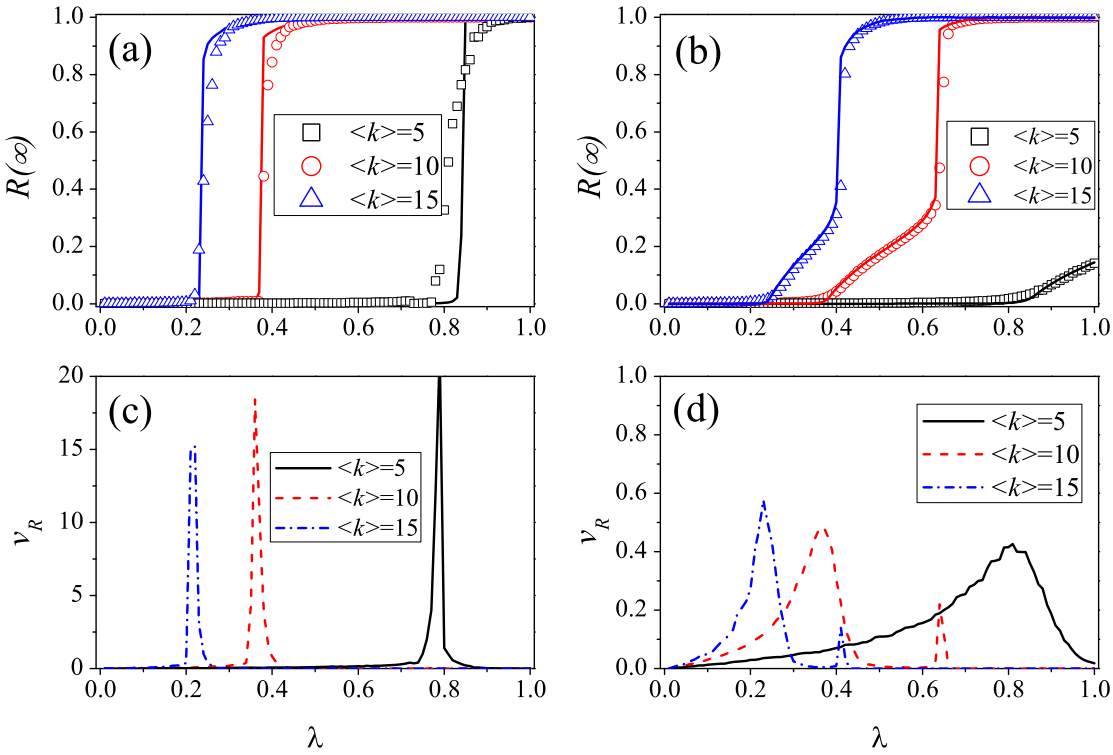

Figure 8. Effects of mean degree on two-state spreading threshold model. For $T_b = 2$, (a) $R(\infty)$ and (c) ν_R versus λ with different $\langle k\rangle$. For $T_b = 4$, (b) $R(\infty)$ and (d) ν_R as a function of λ for different $\langle k\rangle$. In (a) and (b), symbols are the simulated results, and the lines are the theoretical predictions from equations (12)–(14) and (16)–(20). Lines in (c) and (d) are the simulation results of ν_R. We set other parameters to be $N = 10\,000$ and $p = 0.3$.

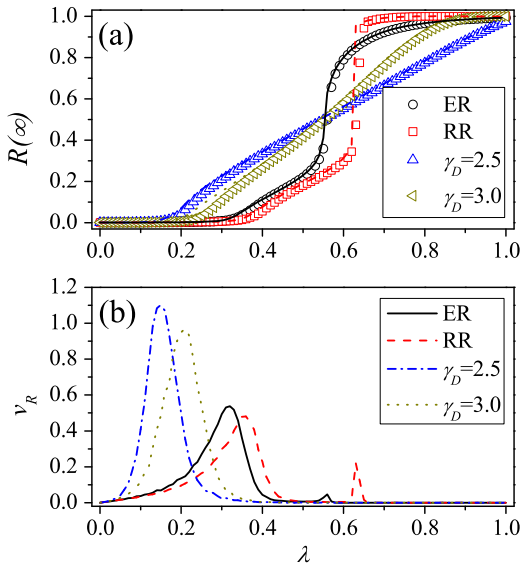

Figure 9. For $T_b = 4$, the effects of network heterogeneity on two-state spreading threshold model. (a) $R(\infty)$ and (b) ν_R versus λ on random regular networks, Erdős–Rényi (ER) networks, and scale-free networks with degree exponent $\gamma_D = 2.5$ and 3.0. In figure (a), symbols represent the simulated results, and the lines are theoretical predictions from equations (12)–(14) and (16)–(20). Lines in (b) are the simulation results of ν_R. We set other parameters to be $N = 10\,000$ and $p = 0.3$.

behavior. Moreover, all the first-order, second-order and hybrid phase transitions are found in the system. For the case of $T_b = 1$, our model reduces to the SIR model, and the traditional second-order phase transition thus arises; for $T_b = 2$, the first phase transition occurs; for $T_b \geqslant 3$, the hybrid phase transition mixed first and second order emerges, i.e., $R(\infty)$ versus λ first grows continuously and then follows by a discontinuous pattern. It can

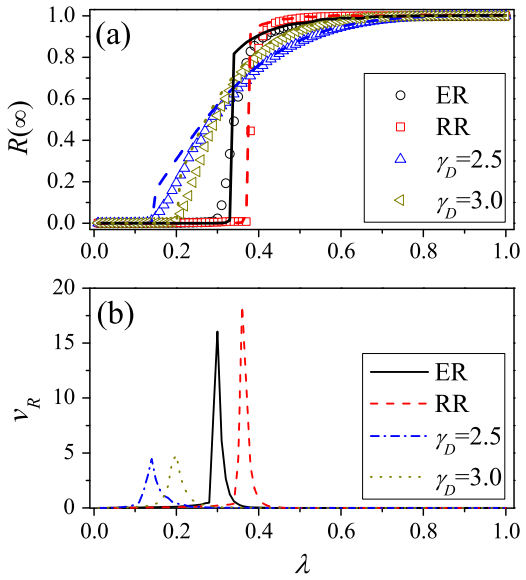

Figure 10. For $T_b = 2$, the effects of network heterogeneity on two-state spreading threshold model. (a) $R(\infty)$ and (b) v_R versus λ on random regular networks, Erdős–Rényi (ER) networks, and scale-free networks with degree exponent $\gamma_D = 2.5$ and 3.0. In figure (a), symbols represent the simulated results, and the lines are the theoretical predictions from equations (12)–(14) and (16)–(20). Lines in (b) are the simulation results of v_R. And other parameters are set to be $N = 10\,000$ and $p = 0.3$.

be clearly seen that by varying p, two types of crossover phenomena occur in phase transition. Specifically, the phase transition changes from first-order to second-order when $T_b = 2$. For the case of $T_b \geqslant 3$, the phase transition changes from hybrid to second-order.

We found that the structural parameters markedly affect $R(\infty)$ and phase transition. On the one hand, the behavior spreads easier at a large value of $\langle k \rangle$. On RRNs, for a small bigots' adoption threshold, such as $T_b = 2$, the discontinuous phase transition is not altered by varying $\langle k \rangle$. Correspondingly, for a relatively large $T_b = 4$, there is a crossover phenomenon by decreasing $\langle k \rangle$: a hybrid phase transition changes to a continuous phase transition. On the other hand, the network heterogeneity makes the behavior outbreak more easily. For small (large) value of λ, network heterogeneity promotes (suppresses) the adoption of behavior. For a small value of $T_b = 2$, the discontinuous phase transition is not altered by the network heterogeneity; for a large value of $T_b = 4$, a crossover phenomenon occurs by increasing network heterogeneity, i.e., a change from being hybrid phase transition to being second-order phase transition.

The main contribution of our work lies in providing a qualitative and quantitative view on the influence of heterogeneous adoption threshold, and enriching the studies about phase transition phenomenon. Our developed theory can offer new inspirations for other spreading dynamics studies, such as epidemic spreading and cascading. However, some fascinating and hopeful challenges still remain. For example, what will happen if the adoption thresholds are correlated with their degrees? How to extract more realistic behavior spreading mechanisms from real data?

Acknowledgments

This work was partially supported by the National Natural Science Foundation of China under Grants Nos. 11105025, 11575041 and 61433014, the Program of Outstanding PhD Candidate in Academic Research by UESTC under Grand No. YXBSZC20131065.

References

[1] Watts D J and Dodds P S 2007 *J. Consum. Res.* **34** 441
[2] Castellano C, Fortunato S and Fortunato S 2009 *Rev. Mod. Phys.* **81** 0034
[3] Christakis N A and Fowler J H 2007 *N. Engl. J. Med.* **357** 370
[4] Barrat A, Barthélemy M and Vespignani A 2007 *Dynamical Processes on Complex Networks* (Cambridge: Cambridge University Press)
[5] Centola D 2011 *Science* **334** 1269
[6] Banerjee A, Chandrasekhar A G, Duflo E and Jackson M O 2013 *Science* **341** 363
[7] Pastor-Satorras R, Castellano C, Mieghem P V and Vespignani A 2015 *Rev. Mod. Phys.* **87** 925
[8] Moreno Y, Pastor-Satorras R and Vespignani A 2002 *Eur. Phys. J.* B **26** 521

[9] Pastor-Satorras R and Vespignani A 2001 *Phys. Rev. Lett.* **86** 3200
[10] Salathé M and Khandelwal S 2011 *PLoS Comput. Biol.* **7** e1002199
[11] Yang H X, Tang M and Lai Y C 2015 *Phys. Rev.* E **91** 062817
[12] Yang H X, Wang W X, Lai Y C, Xie Y B and Wang B H 2011 *Phys. Rev.* E **84** 045101(R)
[13] Li K, Fu X, Small M and Zhu G 2014 *Chaos* **24** 043124
[14] Porter M A and Gleeson J P 2014 arXiv:1403.7663v1
[15] Watts D J 2002 *Proc. Natl Acad. Sci.* **99** 5766
[16] Granovetter M 1973 *Am. J. Sociol.* **78** 1360
[17] Gleeson J P and Cahalane D J 2007 *Phys. Rev.* E **75** 056103
[18] Singh P, Sreenivasan S, Szymanski B K and Korniss G 2013 *Sci. Rep.* **3** 2330
[19] Dodds P S and Payne J L 2009 *Phys. Rev.* E **79** 066115
[20] Whitney D E 2010 *Phys. Rev.* E **82** 066110
[21] Gleeson J P 2008 *Phys. Rev.* E **77** 046117
[22] Nematzadeh A, Ferrara E, Flammini A and Ahn Y Y 2014 *Phys. Rev. Lett.* **113** 088701
[23] Brummitt C D, Lee K-M and Goh K-I 2012 *Phys. Rev.* E **85** 045102(R)
[24] Yağan O and Gligor V 2013 *Phys. Rev.* E **86** 036103
[25] Dodds P S and Watts D J 2004 *Phys. Rev. Lett.* **92** 218701
[26] Wang W, Tang M, Zhang H-F and Lai Y-C 2015 *Phys. Rev.* E **92** 012820
[27] Zheng M, Lü L and Zhao M 2013 *Phys. Rev.* E **88** 012818
[28] Centola D 2010 *Science* **329** 1194
[29] Miller J C 2007 *Phys. Rev.* E **76** 010101
[30] Yang H, Tang M and Gross T 2015 *Sci. Rep.* **5** 13122
[31] Cui A-X, Wang W, Tang M, Fu Y, Liang X and Do Y 2014 *Chaos* **24** 033113
[32] Jo H H, Perotti J I, Kaski K and Kertész J 2014 *Phys. Rev.* X **4** 011041
[33] Wu C, Ji S, Zhang R, Chen L, Chen J, Li X and Hu Y 2014 *Europhys. Lett.* **107** 48001
[34] Hu Y, Ksherim B, Cohen R and Havlin S 2011 *Phys. Rev.* E **84** 066116
[35] Cellai D, Lawlor A, Dawson K A and Gleeson J P 2011 *Phys. Rev. Lett.* **107** 175703
[36] Baxter G J, Dorogovtsev S N, Goltsev A V and Mendes J F F 2011 *Phys. Rev.* E **83** 051134
[37] Lee K-M, Brummitt C D and Goh K-I 2014 *Phys. Rev.* E **90** 062816
[38] Karsai M, Iñiguez G, Kaski K and Kertész J 2014 *J. R. Soc. Interface* **11** 101
[39] Catanzaro M, Boguñá M and Pastor-Satorras R 2005 *Phys. Rev.* E **71** 027103
[40] Wang W, Shu P-P, Zhu Y-X, Tang M and Zhang Y-C 2015 *Chaos* **25** 103102
[41] Miller J C, Slim A C and Volz E M 2012 *J. R. Soc. Interface* **9** 890
[42] Miller J C and Volz E M 2013 *PLoS One* **8** e69162
[43] Wang W, Tang M, Zhang H-F, Gao H, Do Y and Liu Z-H 2014 *Phys. Rev.* E **90** 042803
[44] Karrer B and Newman M E J 2010 *Phys. Rev.* E **82** 016101
[45] Newman M E J, Strogatz S H and Watts D J 2001 *Phys. Rev.* E **64** 026118
[46] Strogatz S H 1994 *Nonlinear Dynamics and Chaos: With Applications to Physics, Biology, Chemistry and Engineering* (Boulder, CO: Westview)
[47] Dorogovtsev S N, Goltsev A V and Mendes J F F 2008 *Rev. Mod. Phys.* **80** 1275
[48] Chen W, Schröder M and D'Souza M R 2014 *Phys. Rev. Lett.* **112** 155701
[49] Holme P, Kim B J, Yoon C N and Han S K 2002 *Phys. Rev.* E **65** 056109